

Modeling of Emission and Absorption Spectra of LH2 Complex (B850 and B800 Ring) - Full Hamiltonian Model

Pavel Heřman, David Zapletal

Abstract—Simulated absorption and steady state fluorescence spectra for the model of peripheral cyclic antenna unit LH2 from purple bacteria are presented. The spectra for more complex system (B850 and B800 ring) are calculated within full Hamiltonian model and these results are compared with the previous ones calculated within the nearest neighbour approximation model. Dynamic disorder, interaction with phonon bath, in Markovian approximation simultaneously with uncorrelated static disorder in local excitation energies are taken into account in our simulations. The cumulant-expansion method of Mukamel et al. is used for the calculation of spectral responses of the system with exciton-phonon coupling. The localization of exciton states is also investigated.

Keywords—LH2, B800 ring, B850 ring, absorption and fluorescence spectrum, static and dynamic disorder, exciton states, localization

I. INTRODUCTION

IN the process of photosynthesis (in plants, bacteria, and blue-green algae), solar energy is used to split water and produce oxygen molecules, protons and electrons. Nowadays, the photovoltaic systems are widely used to harvest solar energy and transform it into electricity. But the disadvantage of this form of energy is a problem with its storage. The solution could be to convert solar energy into chemical energy as hydrogen, which is easier to store than electricity. For this purpose, it is necessary to construct an effective artificial photosynthetic system [1]–[4]. Such system is not possible to be constructed without detailed knowledge of natural photosynthetic systems. Contribution to better understanding of the structure, properties and function of these systems can be

given also by computer simulations of processes that take place there. Our interest is mainly focused on first (light) stage of photosynthesis in purple bacteria. Solar photon is absorbed by a complex system of membrane-associated pigment-proteins (light-harvesting (LH) antenna) and absorbed energy is efficiently transferred to a reaction center (RC), where it is converted into a chemical energy [5].

The antenna systems of photosynthetic units from purple bacteria are formed by ring units LH1, LH2, LH3, and LH4. Their geometric structures are known in great detail from X-ray crystallography [6]–[10]. The general organization of above mentioned light-harvesting complexes is the same: identical subunits are repeated cyclically in such a way that a ring-shaped structure is formed. However the symmetries of these rings are different.

The bacteriochlorophyll (BChl) molecules from LH2 complex in purple bacterium *Rhodospseudomonas acidophila* are organized in two concentric rings. One ring features a group of nine well-separated BChl molecules (B800) with absorption band at about 800 nm. The other ring consists of eighteen closely packed BChl molecules (B850) absorbing around 850 nm. As in B850 ring as in B800 ring dipole moments of bacteriochlorophyll molecules are oriented approximately tangentially to corresponding ring. While the nearest neighbour dipole moments in B850 ring have antiparallel arrangement, in B800 ring the orientations of the nearest neighbour dipole moments are parallel [11]. LH2 complexes from other purple bacteria have analogous ring structure.

Some bacteria express also other types of complexes such as the B800-820 LH3 complex (*Rhodospseudomonas acidophila* strain 7050) or the LH4 complex (*Rhodospseudomonas palustris*). LH3 complex like LH2 one is usually nonameric but LH4 one is octameric. The other difference is the presence of an additional BChl ring in LH4 complex [8]. Different arrangements manifest themselves in different optical properties. At this article we mainly focus on LH2 complex.

Despite intensive study of bacterial antenna systems, e.g. [6]–[8], [12], the precise role of the protein moiety for governing the dynamics of the excited states is still under debate. At room temperature the solvent and protein environment fluctuates with characteristic time

Manuscript received November , 2015.

This work was supported in part by the Faculty of Science, University of Hradec Králové (project of specific research No. 2106/2015 - P. Heřman).

P. Heřman is with the Department of Physics, Faculty of Science, University of Hradec Králové, Rokitsanského 62, 50003 Hradec Králové, Czech Republic (e-mail: pavel.herman@uhk.cz).

D. Zapletal is with the Institute of Mathematics and Quantitative Methods, Faculty of Economics and Administration, University of Pardubice, Studentská 95, 53210 Pardubice, Czech Republic (e-mail: david.zapletal@upce.cz).

scales ranging from femtoseconds to nanoseconds. The simplest approach is to substitute fast fluctuations by dynamic disorder and slow fluctuations by static disorder.

In our previous papers we presented results of simulations for B850 ring from LH2 complex. In several steps we extended the former investigations of static disorder effect on the anisotropy of fluorescence made by Kumble and Hochstrasser [13] and Nagarajan et al. [14]–[16] for LH2 ring. After studying the influence of diagonal dynamic disorder for simple systems (dimer, trimer) [17]–[19], we added this effect into our model of LH2 ring by using a quantum master equation in Markovian and non-Markovian limits [20]–[22]. We also studied influence of four types of uncorrelated static disorder [23], [24] (Gaussian disorder in local excitation energies, Gaussian disorder in transfer integrals, Gaussian disorder in radial positions of bacteriochlorophyll molecules on the ring and Gaussian disorder in angular positions of bacteriochlorophyll molecules on the ring). Influence of correlated static disorder, namely an elliptical deformation of the ring, was also taken into account [20]. We also investigated the time dependence of fluorescence anisotropy for the LH4 ring with different types of uncorrelated static disorder [22], [25].

Recently we have focused on the modeling of absorption and steady state fluorescence spectra. Our results for B850 ring from LH2 complex and B- α /B- β ring from LH4 complex within the nearest neighbour approximation (NN) model have been presented in [26]–[31]. The results within full Hamiltonian (FH) model were published in [32]–[39].

Main goal of the present paper is the comparison of the results for full LH2 complex (B850 ring and B800 ring) calculated within full Hamiltonian model with our previous results [40] calculated within the nearest neighbour approximation model. The rest of the paper is organized as follows. Section 2 introduces the ring model with the static disorder and dynamic disorder (interaction with phonon bath), the cumulant expansion method, which is used for the calculation of spectral responses of the system with exciton-phonon coupling, and also formulas for assessment of exciton states localization. Computational point of view is mentioned in Section 3. The presented results of our simulations, used units and parameters could be found in Section 4, some conclusions are drawn in Section 5.

II. PHYSICAL MODEL

We assume that only one excitation is present on the ring complex after an impulsive excitation. The Hamiltonian of an exciton in the ideal ring complex coupled to a bath of harmonic oscillators reads

$$H = H_{\text{ex}}^0 + H_s + H_{\text{ph}} + H_{\text{ex-ph}}. \quad (1)$$

First term,

$$H_{\text{ex}}^0 = \sum_{m,n(m \neq n)} J_{mn} a_m^\dagger a_n, \quad (2)$$

corresponds to an exciton, e.g. the system without any disorder. The operator a_m^\dagger (a_m) creates (annihilates) an exciton at site m , J_{mn} (for $m \neq n$) is the so-called transfer integral between sites m and n .

Both rings (B850 and B800) can be modeled as homogeneous cases. If the nearest neighbour approximation is used (only the nearest neighbour transfer matrix elements are nonzero), the transfer integrals in B850 ring and B800 one read

$$J_{mn}^{\text{B850}} = J_0(\delta_{m,n+1} + \delta_{m,n-1}), \quad m, n = 1, \dots, 18, \quad (3)$$

$$J_{mn}^{\text{B800}} = J_1(\delta_{m,n+1} + \delta_{m,n-1}), \quad m, n = 19, \dots, 27. \quad (4)$$

Due to orientations of dipole moments [11], sign of J_0 is positive and J_1 is negative and the relation between them is given by the following equation

$$J_1 = -0.1J_0. \quad (5)$$

Each bacteriochlorophyll molecule from B800 ring is connected by nonzero transferintegrals with two nearest neighbour bacteriochlorophyll molecules from B850 ring. These transferintegrals have opposite signs. Their values are

$$J_{1,19} = J_{3,20} = \dots = J_{17,27} = 0.1J_0, \quad (6)$$

$$J_{2,19} = J_{4,20} = \dots = J_{18,27} = -0.03J_0. \quad (7)$$

If all interactions between bacteriochlorophylls are taking into account (all off-diagonal matrix elements of Hamiltonian are nonzero), geometrical arrangement of the complex has to be carefully examined. It is necessary that the nearest neighbour matrix elements within full Hamiltonian model (in dipole-dipole approximation) have the same values as in the nearest neighbour approximation model.

The pure exciton hamiltonian H_{ex}^0 can be diagonalized using the wave vector representation with corresponding delocalized Bloch states α and energies E_α . Using Fourier transformed excitonic operators a_α , the Hamiltonian H_{ex}^0 in α -representation reads

$$H_{\text{ex}}^0 = \sum_{\alpha} E_{\alpha} a_{\alpha}^{\dagger} a_{\alpha}. \quad (8)$$

If we consider only one ring (B850 or B800) separately within the nearest neighbour approximation model, the form of operators a_α in Eq. (8) is

$$a_{\alpha} = \sum_{n=1}^N a_n e^{i\alpha n}, \quad \alpha = \frac{2\pi}{N}l. \quad (9)$$

Energies E_α are

$$E_{\alpha} = -2J_0 \cos \alpha \quad (10)$$

for B850 ring and

$$E_\alpha = -2J_1 \cos \alpha \quad (11)$$

for B800 ring. Here

$$l = 0, \pm 1, \dots, \pm \frac{N}{2} \quad (12)$$

for even number of sites N (i.e. for B850 ring $N = 18$) and

$$l = 0, \pm 1, \dots, \pm \frac{N-1}{2} \quad (13)$$

for odd number of sites N (i.e. for B800 ring $N = 9$). If both rings are considered simultaneously, energetic spectrum is more complex. In Figure 1 the differences between the spectrum within full Hamiltonian model (left column) and that one within the nearest neighbour approximation model (right column) can be seen.

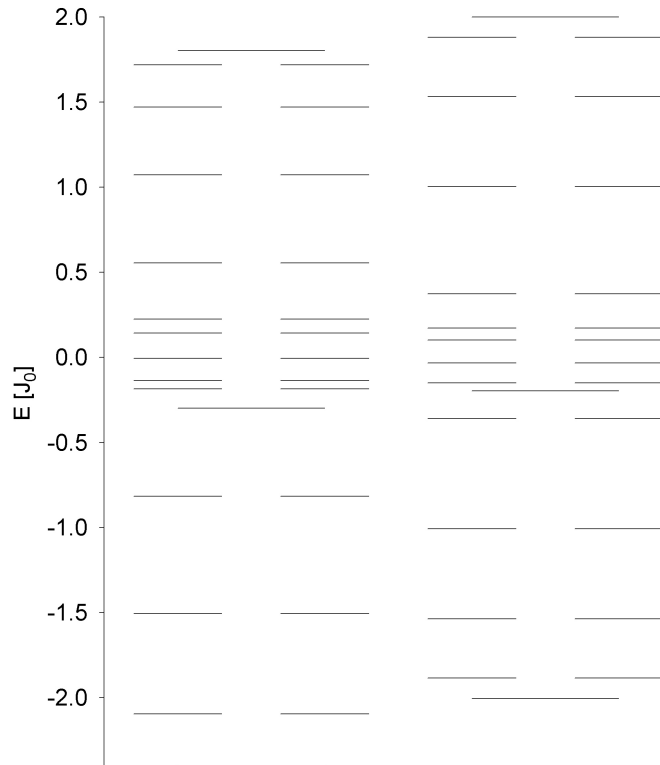


Fig. 1. Energetic band structure for full LH2 complex - B850 ring and B800 ring (full Hamiltonian (FH) model - left column, the nearest neighbour (NN) model - right column).

Influence of static disorder (second term in Eq. (1)) is modeled by totally uncorrelated fluctuations of local excitation energies $\delta\varepsilon_n$ with Gaussian distribution and standard deviation Δ . Hamiltonian of static disorder H_s then reads

$$H_s = \sum_n \delta\varepsilon_n a_n^\dagger a_n. \quad (14)$$

The third term in Eq. (1),

$$H_{\text{ph}} = \sum_q \hbar\omega_q b_q^\dagger b_q, \quad (15)$$

represents phonon bath in harmonic approximation (the phonon creation and annihilation operators are denoted by b_q^\dagger and b_q , respectively).

Last term in Eq. (1),

$$H_{\text{ex-ph}} = \frac{1}{\sqrt{N}} \sum_m \sum_q G_q^m \hbar\omega_q a_m^\dagger a_m (b_q^\dagger + b_q), \quad (16)$$

describes exciton-phonon interaction which is assumed to be site-diagonal and linear in the bath coordinates (the term G_q^m denotes the exciton-phonon coupling constant).

The cumulant-expansion method of Mukamel et al. [41], [42] is used for the calculation of spectral responses of the system with exciton-phonon coupling. Absorption $OD(\omega)$ and steady-state fluorescence $FL(\omega)$ spectrum can be expressed as

$$OD(\omega) = \omega \sum_\alpha d_\alpha^2 \times \text{Re} \int_0^\infty dt e^{i(\omega - \omega_\alpha)t - g_{\alpha\alpha\alpha\alpha}(t) - R_{\alpha\alpha\alpha\alpha}t}, \quad (17)$$

$$FL(\omega) = \omega \sum_\alpha P_\alpha d_\alpha^2 \times \text{Re} \int_0^\infty dt e^{i(\omega - \omega_\alpha)t + i\lambda_{\alpha\alpha\alpha\alpha}t - g_{\alpha\alpha\alpha\alpha}^*(t) - R_{\alpha\alpha\alpha\alpha}t}. \quad (18)$$

Here $\vec{d}_\alpha = \sum_n c_n^\alpha \vec{d}_n$ is the transition dipole moment of the eigenstate α , c_n^α are the expansion coefficients of the eigenstate α in site representation and P_α is the steady state population of the eigenstate α . The inverse lifetime of exciton state α ($R_{\alpha\alpha\alpha\alpha}$) [43] is given by the elements of Redfield tensor $R_{\alpha\beta\gamma\delta}$ [44]. $R_{\alpha\alpha\alpha\alpha}$ is a sum of the relaxation rates between exciton states,

$$R_{\alpha\alpha\alpha\alpha} = - \sum_{\beta \neq \alpha} R_{\beta\beta\alpha\alpha}.$$

The g-function and λ -values in Eq. (18) are given by

$$g_{\alpha\beta\gamma\delta} = - \int_{-\infty}^\infty \frac{d\omega}{2\pi\omega^2} C_{\alpha\beta\gamma\delta}(\omega) \times \left[\coth \frac{\omega}{2k_B T} (\cos \omega t - 1) - i(\sin \omega t - \omega t) \right], \quad (19)$$

$$\lambda_{\alpha\beta\gamma\delta} = - \lim_{t \rightarrow \infty} \frac{d}{dt} \text{Im} \{ g_{\alpha\beta\gamma\delta}(t) \} = \int_{-\infty}^\infty \frac{d\omega}{2\pi\omega} C_{\alpha\beta\gamma\delta}(\omega). \quad (20)$$

The matrix of spectral densities $C_{\alpha\beta\gamma\delta}(\omega)$ in the eigenstate (exciton) representation reflects one-exciton states coupling to the manifold of nuclear modes. In what follows only a diagonal exciton-phonon interaction in site

representation is used (see Eq. (1)), i.e., only fluctuations of the pigment site energies are assumed and the restriction to the completely uncorrelated dynamic disorder is applied. In such case each site (i.e. each chromophore) has its own bath completely uncoupled from the baths of the other sites. Furthermore it is assumed that these baths have identical properties [21], [45], [46]

$$C_{mnm'n'}(\omega) = \delta_{mn}\delta_{mm'}\delta_{nn'}C(\omega) \quad (21)$$

and we have only one spectral density function $C(\omega)$. After transformation to the exciton representation Eq. (21) reads

$$C_{\alpha\beta\gamma\delta}(\omega) = \sum_n c_n^\alpha c_n^\beta c_n^\gamma c_n^\delta C(\omega). \quad (22)$$

Various models of spectral density of the bath are used in literature [43], [47], [48]. In our present investigation we have used the model of Kühn and May [47]

$$C(\omega) = \Theta(\omega)j_0 \frac{\omega^2}{2\omega_c^3} e^{-\omega/\omega_c}. \quad (23)$$

Here j_0 is the strength of exciton-phonon interaction and ω_c is so called cut-off frequency. Spectral density function $C(\omega)$ has its maximum at $2\omega_c$.

Localization of the exciton states contributing to the steady state fluorescence spectrum can be characterized by the thermally averaged participation ratio $\langle PR \rangle$, which is given by

$$\langle PR \rangle = \frac{\sum_\alpha PR_\alpha e^{-\frac{E_\alpha}{k_B T}}}{\sum_\alpha e^{-\frac{E_\alpha}{k_B T}}}, \quad (24)$$

where

$$PR_\alpha = \sum_{n=1}^N |c_n^\alpha|^4. \quad (25)$$

III. COMPUTATIONAL POINT OF VIEW

To obtain absorption and steady state fluorescence spectra it is necessary to calculate single ring $OD(\omega)$ and $FL(\omega)$ spectra for large number of different static disorder realizations created by random number generator. Finally these results have to be averaged over all realizations of static disorder.

For calculations of spectral responses a procedure created by us in Fortran was used. Integrated functions are oscillating and damped (see Eq. (17) and Eq. (18)) and function $\text{Re } g_{\alpha\alpha\alpha\alpha}(t)$ is non-negative. Therefore absolute values of them (for individual α) satisfy inequalities [38]

$$\left| \text{Re} \left\{ e^{i(\omega-\omega_\alpha)t - g_{\alpha\alpha\alpha\alpha}(t) - R_{\alpha\alpha\alpha\alpha}t} \right\} \right| \leq e^{-R_{\alpha\alpha\alpha\alpha}t}, \quad (26)$$

$$\left| \text{Re} \left\{ e^{i(\omega-\omega_\alpha)t + i\lambda_{\alpha\alpha\alpha\alpha}t - g_{\alpha\alpha\alpha\alpha}^*(t) - R_{\alpha\alpha\alpha\alpha}t} \right\} \right| \leq e^{-R_{\alpha\alpha\alpha\alpha}t}. \quad (27)$$

The whole $OD(\omega)$ and $FL(\omega)$ then satisfy

$$OD(\omega) \leq \omega \sum_\alpha d_\alpha^2 \int_0^\infty dt e^{-R_{\alpha\alpha\alpha\alpha}t}, \quad (28)$$

$$\begin{aligned} FL(\omega) &\leq \omega \sum_\alpha P_\alpha d_\alpha^2 \int_0^\infty dt e^{-R_{\alpha\alpha\alpha\alpha}t} \\ &\leq \omega \sum_\alpha d_\alpha^2 \int_0^\infty dt e^{-R_{\alpha\alpha\alpha\alpha}t}. \end{aligned} \quad (29)$$

Predetermined accuracy could be achieved by integration over finite time interval $t \in \langle 0, t_0 \rangle$ (instead of $\langle 0, \infty \rangle$). If

$$t_0 \geq \max \{t_\alpha\}, \quad \alpha = 1, \dots, 27, \quad (30)$$

where t_α satisfy condition (Q is arbitrary real positive number)

$$\begin{aligned} d_\alpha^2 \left[\int_0^\infty dt e^{-R_{\alpha\alpha\alpha\alpha}t} - \int_0^{t_\alpha} dt e^{-R_{\alpha\alpha\alpha\alpha}t} \right] &= \\ &= d_\alpha^2 \frac{e^{-R_{\alpha\alpha\alpha\alpha}t_\alpha}}{R_{\alpha\alpha\alpha\alpha}} \leq \frac{Q}{27\omega}, \end{aligned} \quad (31)$$

i.e.

$$t_\alpha \geq \frac{1}{R_{\alpha\alpha\alpha\alpha}} \ln \left(\frac{27\omega d_\alpha^2}{QR_{\alpha\alpha\alpha\alpha}} \right), \quad (32)$$

then deviations of $OD(\omega)$ and $FL(\omega)$ from precise values are not larger than Q . $OD(\omega)$ and $FL(\omega)$ are therefore integrated as sums of contributions from individual cycles of oscillation. These contributions are added until upper limit of integration exceeds t_0 .

IV. RESULTS

Above mentioned type of uncorrelated static disorder, e.g. fluctuations of local excitation energies $\delta\varepsilon_n$, has been taken into account in our simulations simultaneously with dynamic disorder in Markovian approximation. Resulting absorption and steady state fluorescence spectra for full LH2 complex (B850 ring and B800 ring) calculated within full Hamiltonian model are presented and compared with our previous results calculated within the nearest neighbour approximation model.

Dimensionless energies normalized to J_0 (the transfer integral between the nearest neighbour bacteriochlorophylls in B850 ring from LH2 complex - see Eq. (3)) have been used. Estimation of J_0 varies in literature between 250 cm^{-1} and 400 cm^{-1} . All our simulations of LH2 spectra have been done with the same values of J_0 and unperturbed transition energy from the ground state E_0 ,

$$J_0 = 370 \text{ cm}^{-1}, \quad E_0 = 12280 \text{ cm}^{-1}, \quad (33)$$

that we found for B850 ring from LH2 complex for this type of static disorder [27] and the nearest neighbour approximation model. The value of J_1 (the nearest

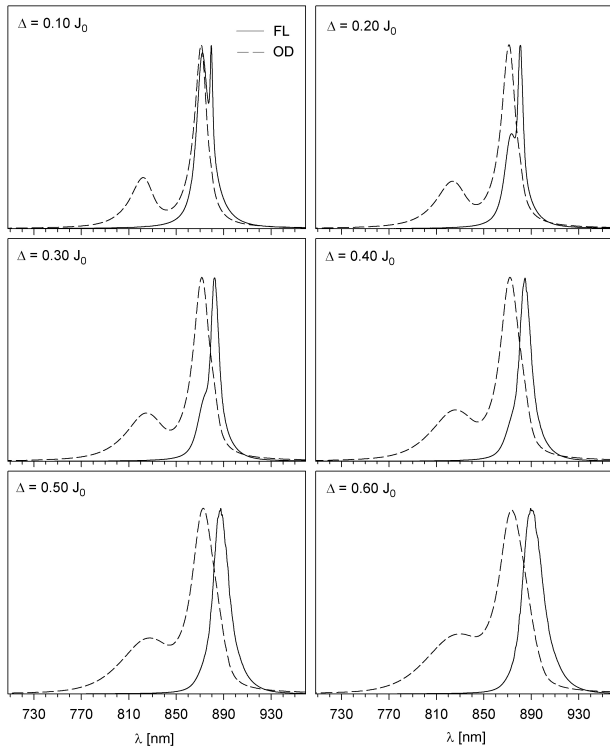


Fig. 2. Calculated *FL* and *OD* spectral profiles (arbitrary units) for full LH2 complex (B850 ring and B800 ring) at low temperature $kT = 0.1 J_0$ averaged over 2000 realizations of uncorrelated static disorder in local excitation energies $\delta\varepsilon_n$ (six strengths $\Delta = 0.10, \dots, 0.60 J_0$), FH model.

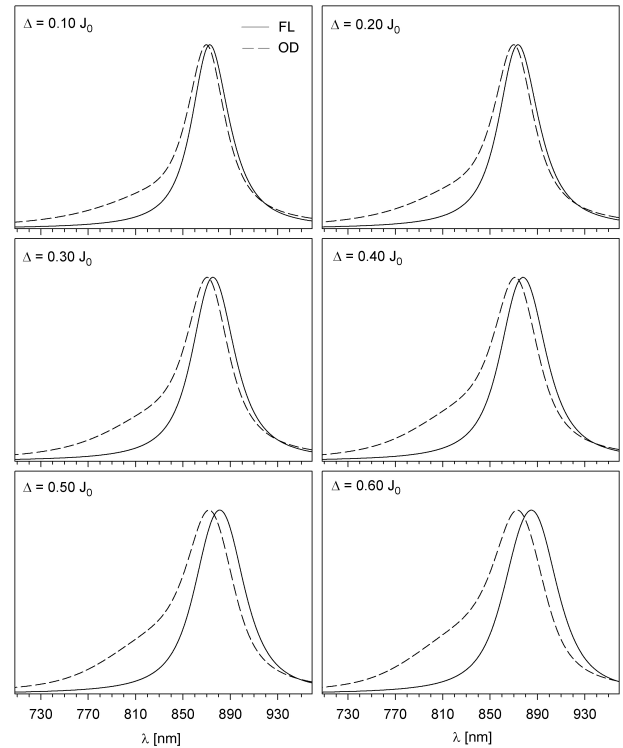


Fig. 3. Calculated *FL* and *OD* spectral profiles (arbitrary units) for full LH2 complex (B850 ring and B800 ring) at room temperature $kT = 0.5 J_0$ averaged over 2000 realizations of uncorrelated static disorder in local excitation energies $\delta\varepsilon_n$ (six strengths $\Delta = 0.10, \dots, 0.60 J_0$), FH model.

neighbour transfer integral in B800 ring - see Eq. (4) and Eq. (5)) is approximately

$$J_1 \doteq -37 \text{ cm}^{-1}. \quad (34)$$

The nearest neighbour transfer integrals connecting bacteriochlorophylls from B850 ring with those from B800 ring have following values (see Eq. (6) and Eq. (7)):

$$J_{1,19} = J_{3,20} = \dots = J_{17,27} \doteq 37 \text{ cm}^{-1}, \quad (35)$$

$$J_{2,19} = J_{4,20} = \dots = J_{18,27} \doteq -11 \text{ cm}^{-1}. \quad (36)$$

Six strengths Δ of static disorder in local excitation energies $\delta\varepsilon_n$ have been chosen in our calculations,

$$\Delta \in \langle 0.10 J_0, 0.60 J_0 \rangle \quad (37)$$

(in agreement with [49]).

The model of spectral density of Kühn and May [47] has been used in our simulations. In agreement with our previous results [23], [50] we have used the strength of dynamic disorder $j_0 = 0.4 J_0$ and cut-off frequency $\omega_c = 0.212 J_0$ (see Eq. (23)).

Resulting absorption *OD* and steady state fluorescence *FL* spectral profiles as functions of wavelength for full LH2 complex averaged over 2000 realizations of static disorder in local excitation energies $\delta\varepsilon_n$ can be seen in

Fig. 2 for low temperature $kT = 0.1 J_0$ and in Fig. 3 for room temperature $kT = 0.5 J_0$. In addition, the comparison of above mentioned results with the results calculated within NN model [40] is done. Comparison of *OD* spectral profiles is shown in Fig. 4 for low temperature $kT = 0.1 J_0$ and in Fig. 5 for room temperature $kT = 0.5 J_0$. *FL* spectral profiles are compared in Fig. 6 for low temperature $kT = 0.1 J_0$ and in Fig. 7 for room temperature $kT = 0.5 J_0$.

The distributions of the quantity $P_\alpha d_\alpha^2$ (see Eq. 18) are shown in Fig. 8 (low temperature $kT = 0.1 J_0$) and in Fig. 9 (room temperature $kT = 0.5 J_0$) for full Hamiltonian model. For comparison, the same for the nearest neighbour approximation model is presented in Fig. 10 (low temperature $kT = 0.1 J_0$) and in Fig. 11 (room temperature $kT = 0.5 J_0$).

In addition, the localization of exciton states is investigated in our paper. The distributions of thermally averaged participation ratio $\langle PR \rangle$ (see Eq. (24)) for full Hamiltonian model are presented in Fig. 12 (low temperature $kT = 0.1 J_0$) and in Fig. 13 (room temperature $kT = 0.5 J_0$). Again, the same for the nearest neighbour approximation model can be seen in Fig. 14 (low temperature $kT = 0.1 J_0$) and in Fig. 15 (room temperature $kT = 0.5 J_0$).

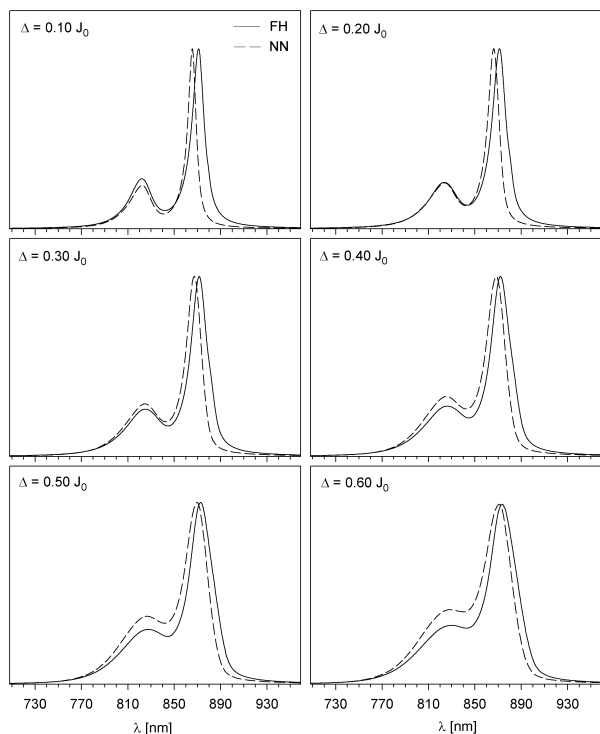


Fig. 4. Comparison of *OD* spectral profiles (arbitrary units) for full LH2 complex calculated within FH model (solid lines) and NN model (dashed lines) at low temperature $kT = 0.1 J_0$ (uncorrelated static disorder in local excitation energies $\delta\varepsilon_n$, $\Delta = 0.10, \dots, 0.60 J_0$).

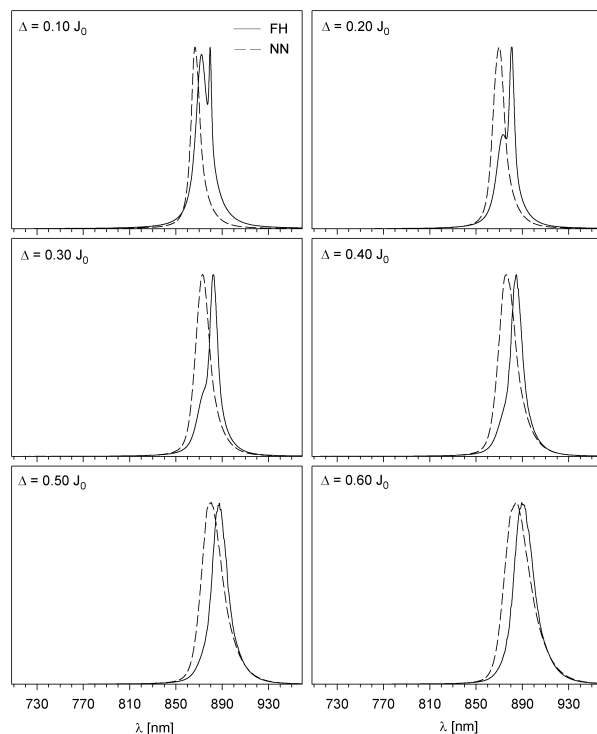


Fig. 6. Comparison of *FL* spectral profiles (arbitrary units) for full LH2 complex calculated within FH model (solid lines) and NN model (dashed lines) at low temperature $kT = 0.1 J_0$ (uncorrelated static disorder in local excitation energies $\delta\varepsilon_n$, $\Delta = 0.10, \dots, 0.60 J_0$).

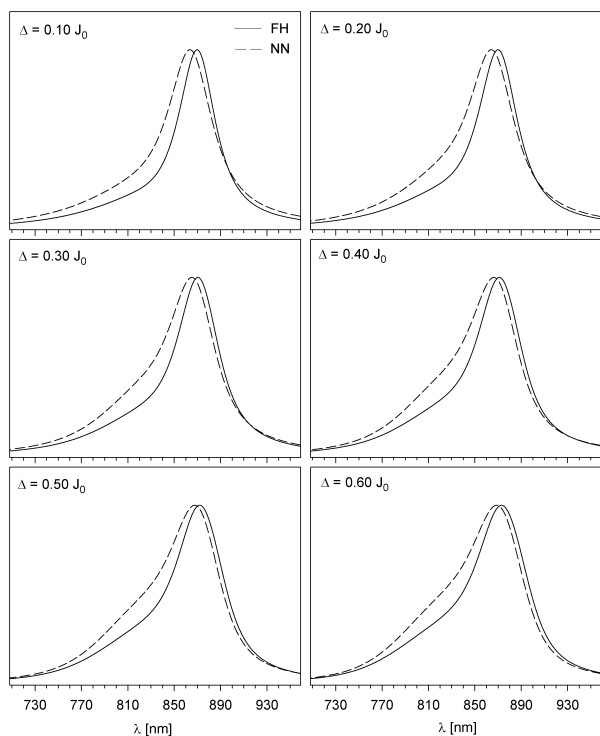


Fig. 5. The same as in Fig. 4 for room temperature $kT = 0.5 J_0$.

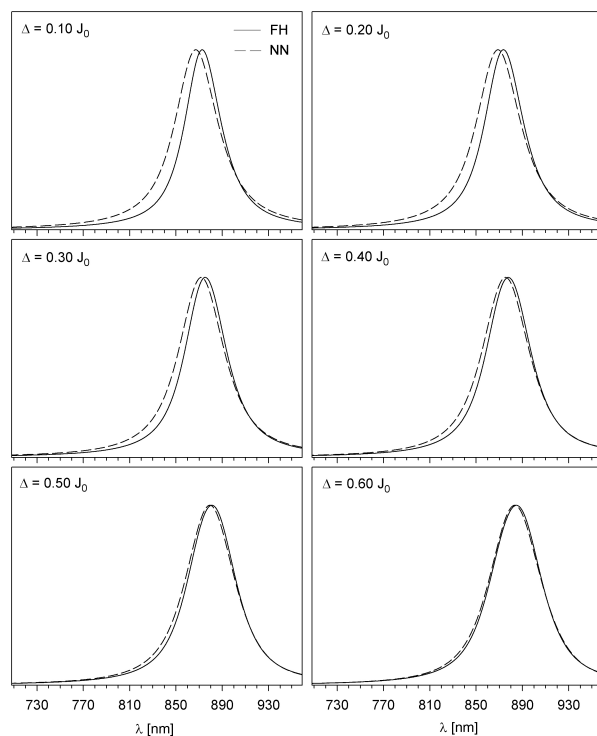


Fig. 7. The same as in Fig. 6 for room temperature $kT = 0.5 J_0$.

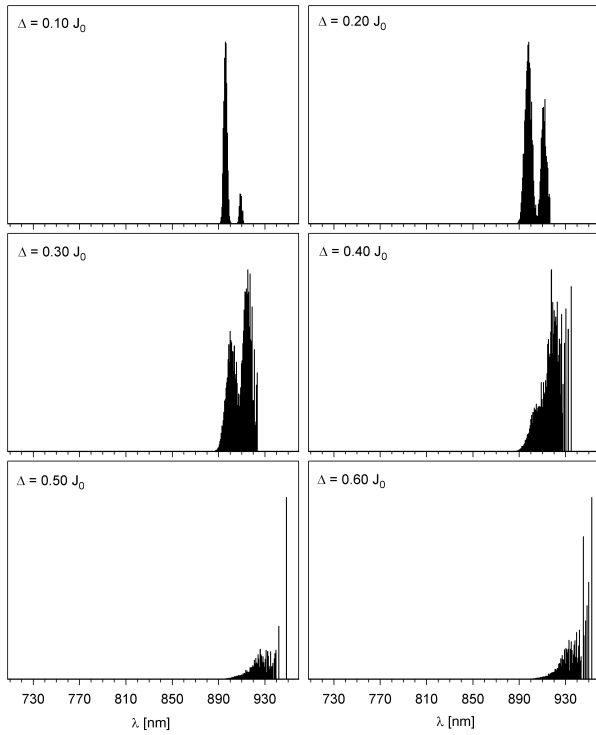


Fig. 8. The distributions of the quantity $P_\alpha d_\alpha^2$ as a function of wavelength λ at low temperature $kT = 0.1 J_0$ for 2000 realizations of uncorrelated static disorder in local excitation energies $\delta\varepsilon_n$ (six strengths $\Delta = 0.1, \dots, 0.6 J_0$), FH model.

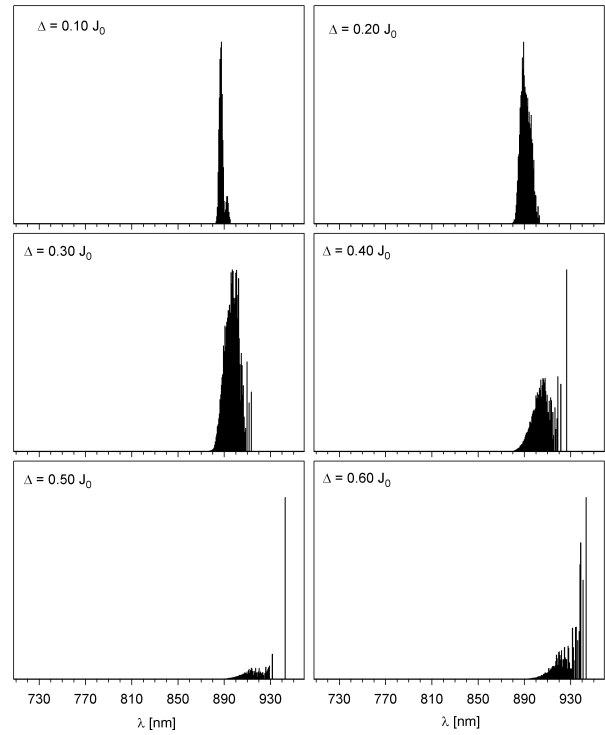


Fig. 10. The distributions of the quantity $P_\alpha d_\alpha^2$ as a function of wavelength λ at low temperature $kT = 0.1 J_0$ for 2000 realizations of uncorrelated static disorder in local excitation energies $\delta\varepsilon_n$ (six strengths $\Delta = 0.1, \dots, 0.6 J_0$), NN model.

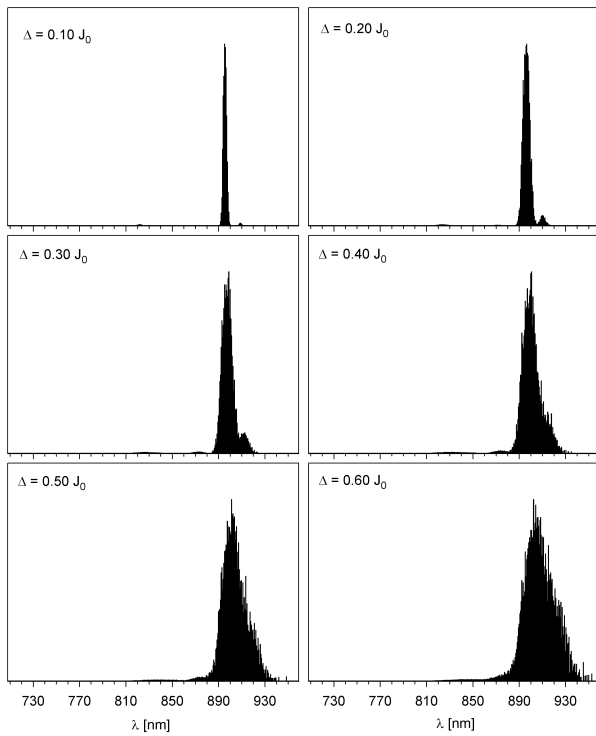


Fig. 9. The same as in Fig. 8 for room temperature $kT = 0.5 J_0$.

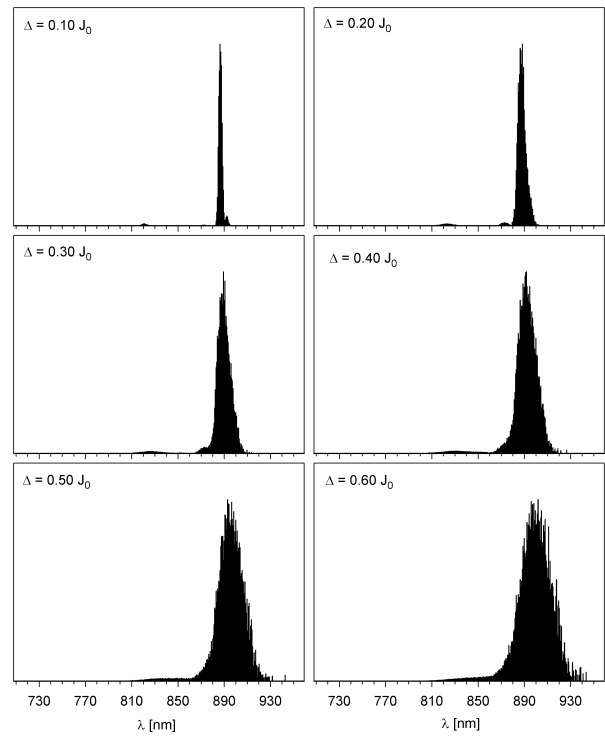


Fig. 11. The same as in Fig. 10 for room temperature $kT = 0.5 J_0$.

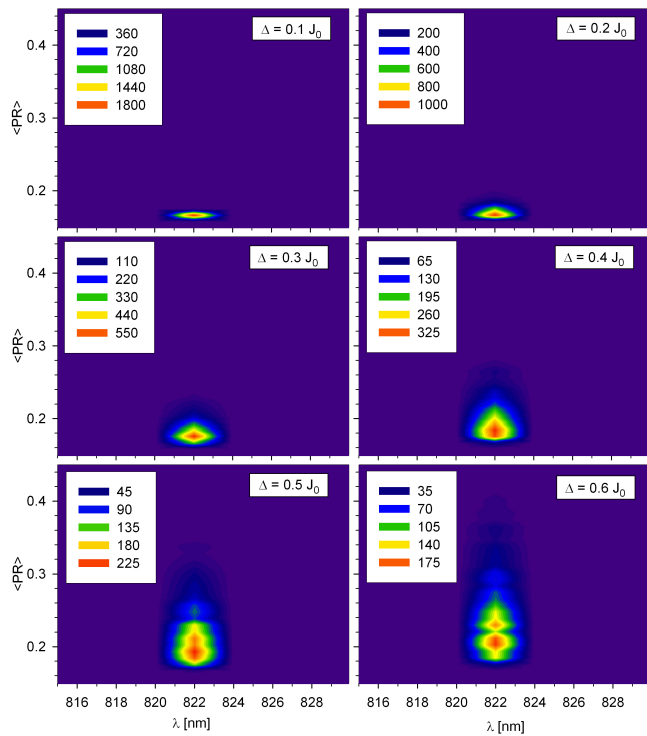


Fig. 12. The distributions of the quantity $\langle PR \rangle$ as a function of FL peak position wavelength at low temperature $kT = 0.1 J_0$ for 2000 realizations of uncorrelated static disorder in local excitation energies $\delta\varepsilon_n$ (six strengths $\Delta = 0.1, \dots, 0.6 J_0$), FH model.

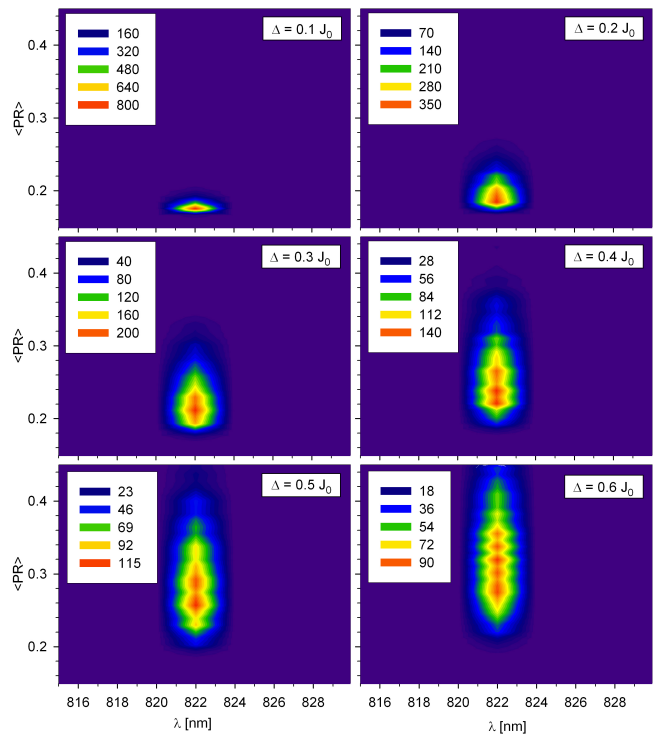


Fig. 14. The distributions of the quantity $\langle PR \rangle$ as a function of FL peak position wavelength at low temperature $kT = 0.1 J_0$ for 2000 realizations of uncorrelated static disorder in local excitation energies $\delta\varepsilon_n$ (six strengths $\Delta = 0.1, \dots, 0.6 J_0$), NN model.

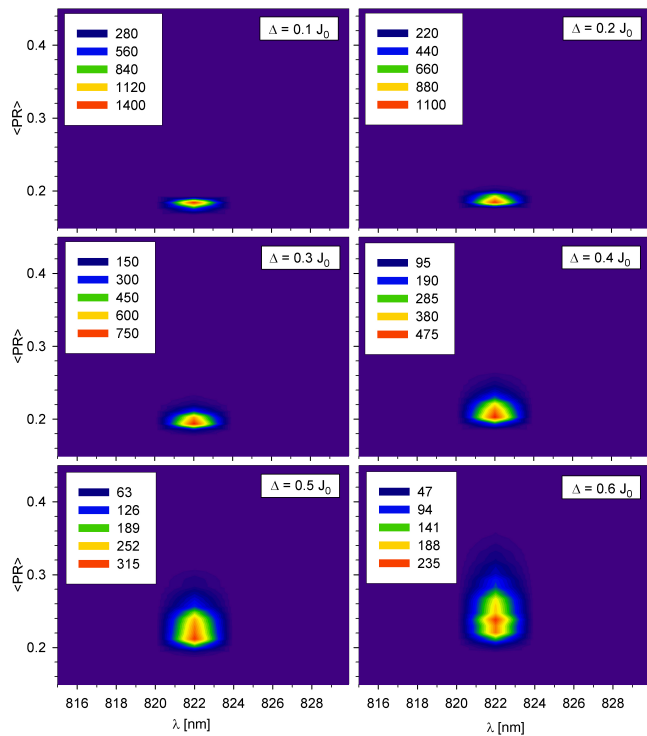


Fig. 13. The same as in Fig. 12 for room temperature $kT = 0.5 J_0$.

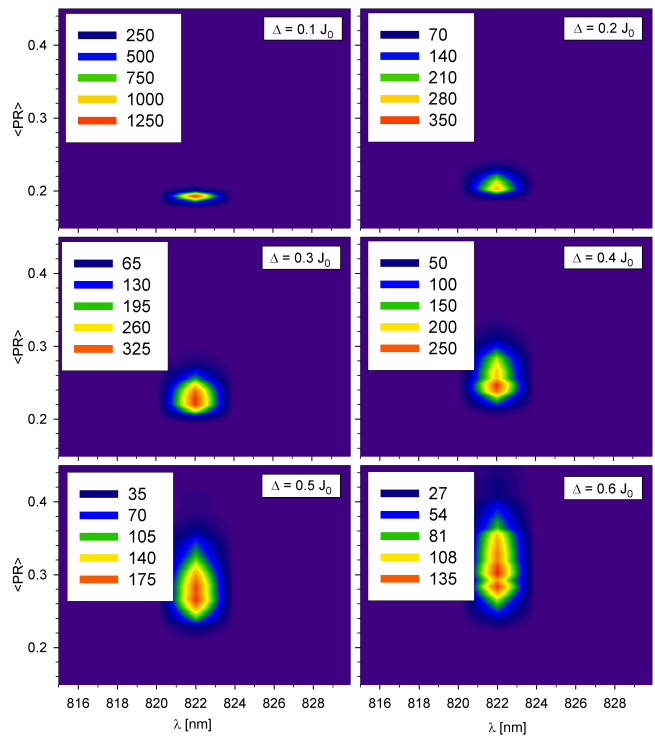


Fig. 15. The same as in Fig. 14 for room temperature $kT = 0.5 J_0$.

V. CONCLUSIONS

From our new results for full LH2 complex calculated within full Hamiltonian model and from comparison with our previous results calculated within the nearest neighbour approximation model we can make following conclusions.

The most important difference between spectral profiles is visible for fluorescence spectrum at low temperature $kT = 0.1 J_0$. Fluorescence spectral line is split in case of full Hamiltonian model (see Fig. 2), contrary to the nearest neighbour approximation one (see Fig. 6). It corresponds to the distributions of the quantity $P_\alpha d_\alpha^2$ (see Figure 8 and Figure 10). The peak position of fluorescence spectral profile in case of full Hamiltonian model is shifted to higher wavelengths in comparison with the case of the nearest neighbour approximation model. On the other hand, any splitting of fluorescence spectral line is not visible at room temperature $kT = 0.5 J_0$ (see Fig. 3). It again corresponds to the distributions of the quantity $P_\alpha d_\alpha^2$ (see Figure 9 and Figure 11). In this case the splitting is hidden due to fluorescence spectral line widening caused by dynamic disorder. The differences in fluorescence spectrum peak positions between both models of Hamiltonian are not so essential at room temperature (see Fig. 7). As for low temperature as for room temperature fluorescence spectral lines are shifted to higher wavelengths with growing strength of static disorder (see Fig. 2 and Fig. 3). This shift is higher in case of the nearest neighbour approximation model (see Fig. 6 and Fig. 7).

Contrary to fluorescence spectrum any shift of absorption spectral line peak with growing strength of static disorder is not visible for both temperatures (see Fig. 2 and Figure 3). But the differences between both models of Hamiltonian in peak positions and widths of spectral lines are evident. Peak positions are again shifted to higher wavelengths in case of full Hamiltonian model in comparison with the nearest neighbour approximation model (see Fig. 4 and Fig. 5). Absorption spectral lines calculated within the nearest neighbour approximation model are wider in comparison with that ones calculated within full Hamiltonian model.

At low temperature, the spectral line splitting is visible as in fluorescence spectrum as in absorption one. But the reasons of these splittings are different. The absorption spectral line splitting is caused by addition of the second (B800) ring to our system and it is present for both models of Hamiltonian (see Fig. 4). Contrary, the fluorescence spectral line splitting is visible only in case of full Hamiltonian model and it is present as for single B850 ring [32] as for full LH2 complex (B850 ring and B800 ring, see Fig. 6).

As concerns localization of exciton states, in case of low temperature ($kT = 0.1 J_0$) the localization is substantially higher (distributions of $\langle PR \rangle$ reach higher

values) as for FH model (see Fig. 12) as for NN model (see Fig. 14) in comparison with room temperature $kT = 0.5 J_0$ (see Fig. 13 and Fig. 15). Only lowest exciton states, that correspond to B850 ring (see Fig. 1), are occupied at low temperature. On the other hand higher exciton states, that correspond B800 ring, are also occupied at room temperature. It causes lower localization in this case. If we compare localization for both models of Hamiltonian, higher localization can be seen in case of NN model.

REFERENCES

- [1] Y. Sun, Ch. Liu, D. C. Grauer, J. Yano, J. R. Long, P. Yang, J. Ch. Chang, "Electrodeposited cobalt-sulfide catalyst for electrochemical and photoelectrochemical hydrogen generation from water", *J. Am. Chem. Soc.* 135, 2013, pp. 17699–17702.
- [2] K. Kalyanasundaram, M. Graetzel, "Artificial photosynthesis: biomimetic approaches to solar energy conversion and storage", *Current Opinion in Biotechnology* 21, 2010, pp. 298-310.
- [3] L. Savage, "Saving solar energy for a rainy day: Artificial photosynthesis", *Optics and Photonics News* 24(2), 2013, pp. 18–25.
- [4] T. Faunce, "Towards a global solar fuels project- Artificial photosynthesis and the transition from anthropocene to sustainocene", *Procedia Engineering* 49, 2012, pp. 348-356.
- [5] R. van Grondelle, V. I. Novoderezhkin, "Energy transfer in photosynthesis: experimental insights and quantitative models", *Phys. Chem. Chem. Phys.* 8, 2003, pp. 793–807.
- [6] G. McDermott, S. M. Prince, A. A. Freer, A. M. Hawthornthwaite-Lawless, M. Z. Papiz, R. J. Cogdell, N. W. Isaacs, "Crystal structure of an integral membrane light-harvesting complex from photosynthetic bacteria", *Nature* 374, 1995, pp. 517–521.
- [7] M. Z. Papiz, S. M. Prince, T. Howard, R. J. Cogdell, N. W. Isaacs, "The structure and thermal motion of the B 800850 LH2 complex from *Rps. acidophila* at 2.0 Å resolution and 100 K: new structural features and functionally relevant motions", *J. Mol. Biol.* 326, 2003, pp. 1523–1538.
- [8] W. P. F. de Ruijter, S. Oellerich, J.-M. Segura, A. M. Lawless, M. Papiz, T. J. Aartsma, "Observation of the Energy-Level Structure of the Low-Light Adapted B800 LH4 Complex by Single-Molecule Spectroscopy", *Biophys. J.* 87, 2004, pp. 3413–3420.
- [9] A.W. Roszak, T.D. Howard, J. Southall, A.T. Gardiner, C.J. Law, N.W. Isaacs, R.J. Cogdell, "Crystal structure of RCLH1 core complex from *Rhodospseudomonas palustris*", *Science* 203, 2003, pp. 1969–1972.
- [10] K. McLuskey, S. M. Prince, R. J. Cogdell, N. W. Isaacs, "The crystallographic structure of the B800-820 LH3 light-harvesting complex from the purple bacteria *Rhodospseudomonas acidophila* strain 7050", *Biochemistry* 40, 2001, pp. 8783–8789.
- [11] O. Kühn, V. Sundström, T. Pullerits, "Fluorescence Depolarization Dynamics in the B850 Complex of Purple Bacteria", *Chemical Physics* 275, 2002, pp. 15–30.
- [12] R. Kumble, R. Hochstrasser, "Disorder-induced exciton scattering in the light-harvesting systems of purple bacteria: Influence on the anisotropy of emission and band → band transitions", *J. Chem. Phys.* 109, 1998, pp. 855–865.
- [13] V. Nagarajan, R. G. Alden, J. C. Williams, W. W. Parson, "Ultrafast exciton relaxation in the B850 antenna complex of *Rhodobacter sphaeroides*", *Proc. Natl. Acad. Sci. USA* 93, 1996, pp. 13774–13779.
- [14] V. Nagarajan, E. T. Johnson, J. C. Williams, W. W. Parson, "Femtosecond pump-probe spectroscopy of the B850 antenna complex of *Rhodobacter sphaeroides* at room temperature", *J. Phys. Chem. B* 103, 1999, pp. 2297–2309.
- [15] V. Nagarajan, W. W. Parson, "Femtosecond fluorescence depletion anisotropy: Application to the B850 antenna complex of *Rhodobacter sphaeroides*", *J. Phys. Chem. B* 104, 2000, pp. 4010–4013.
- [16] V. Čápek, I. Barvík, P. Heřman, "Towards proper parametrization in the exciton transfer and relaxation problem: dimer", *Chem. Phys.* 270, 2001, pp. 141–156.
- [17] P. Heřman, I. Barvík, "Towards proper parametrization in the exciton transfer and relaxation problem. II. Trimer", *Chem. Phys.* 274, 2001, pp. 199–217.
- [18] P. Heřman, I. Barvík, M. Urbanec, "Energy relaxation and transfer in excitonic trimer", *J. Lumin.* 108, 2004, pp. 85–89.

- [19] P. Heřman, U. Kleinekathöfer, I. Barvák, M. Schreiber, "Exciton scattering in light-harvesting systems of purple bacteria", *J. Lumin.* 94-95, 2001, pp. 447-450.
- [20] P. Heřman, I. Barvák, "Non-Markovian effects in the anisotropy of emission in the ring antenna subunits of purple bacteria photosynthetic systems", *Czech. J. Phys.* 53, 2003, pp. 579-605.
- [21] P. Heřman, U. Kleinekathöfer, I. Barvák, M. Schreiber, "Influence of static and dynamic disorder on the anisotropy of emission in the ring antenna subunits of purple bacteria photosynthetic systems", *Chem. Phys.* 275, 2002, pp. 1-13.
- [22] P. Heřman, I. Barvák, "Temperature dependence of the anisotropy of fluorescence in ring molecular systems", *J. Lumin.* 122-123, 2007, pp. 558-561.
- [23] P. Heřman, I. Barvák, "Coherence effects in ring molecular systems", *Phys. Stat. Sol. C* 3, 2006, 3408-3413.
- [24] P. Heřman, D. Zapletal, I. Barvák, "The anisotropy of fluorescence in ring units III: Tangential versus radial dipole arrangement", *J. Lumin.* 128, 2008, pp. 768-770.
- [25] P. Heřman, I. Barvák, D. Zapletal, "Computer simulation of the anisotropy of fluorescence in ring molecular systems: Tangential vs. radial dipole arrangement", *Lecture Notes in Computer Science* 5101, 2008, pp. 661-670.
- [26] P. Heřman, D. Zapletal, J. Šlégr, "Comparison of emission spectra of single LH2 complex for different types of disorder", *Phys. Proc.* 13, 2011, pp. 14-17.
- [27] P. Heřman, D. Zapletal, M. Horák, "Computer simulation of steady state emission and absorption spectra for molecular ring", *Proc. 5th International Conference on Advanced Engineering Computing and Applications in Sciences (ADVCOMP2011)*, Lisbon: IARIA, 2011, pp. 1-6.
- [28] D. Zapletal, P. Heřman, "Simulation of molecular ring emission spectra: localization of exciton states and dynamics", *Int. J. Math. Comp. Sim.* 6, 2012, pp. 144-152.
- [29] M. Horák, P. Heřman, D. Zapletal, "Simulation of molecular ring emission spectra - LH4 complex: localization of exciton states and dynamics", *Int. J. Math. Comp. Sim.* 7, 2013, pp. 85-93.
- [30] M. Horák, P. Heřman, D. Zapletal, "Modeling of emission spectra for molecular rings - LH2, LH4 complexes", *Phys. Proc.* 44, 2013, pp. 10-18.
- [31] P. Heřman, D. Zapletal, "Intermolecular coupling fluctuation effect on absorption and emission spectra for LH4 ring", *Int. J. Math. Comp. Sim.* 7, 2013, pp. 249-257.
- [32] P. Heřman, D. Zapletal, M. Horák, "Emission spectra of LH2 complex: full Hamiltonian model", *Eur. Phys. J. B* 86, 2013, art. no. 215.
- [33] D. Zapletal, P. Heřman, "Photosynthetic Complex LH2 - Absorption and Steady State Fluorescence Spectra", *Proc. of 6th Int. Conf. on Sust. Energy and Env. Protect. (SEEP2013)*, Maribor: University of Maribor, 2013, pp. 284-290.
- [34] P. Heřman, D. Zapletal, "Emission Spectra of LH4 Complex: Full Hamiltonian Model", *Int. J. Math. Comp. Sim.* 7, 2013, pp. 448-455.
- [35] P. Heřman, D. Zapletal, "Simulation of Emission Spectra for LH4 Ring: Intermolecular Coupling Fluctuation Effect", *Int. J. Math. Comp. Sim.* 8, 2014, pp. 73-81.
- [36] D. Zapletal, P. Heřman, "Photosynthetic complex LH2 - Absorption and steady state fluorescence spectra", *Energy* 77, 2014, pp. 212-219.
- [37] P. Heřman, D. Zapletal, P. Kabrhel, "Simulation of emission spectra for LH2 ring: Fluctuations in radial positions of molecules", *Proc. International Conference on Mathematical Models and Methods in Applied Sciences (MMMAS 2014)*, Saint Petersburg, 2014.
- [38] P. Heřman, D. Zapletal, "Computer Simulation of Emission and Absorption Spectra for LH2 Ring", *Computational Problems in Science and Engineering, Lecture Notes in Electrical Engineering* 343, 2015, pp. 221-234.
- [39] P. Heřman, D. Zapletal, "Simulations of Emission Spectra for LH4 Ring - Fluctuations in Radial Positions of Molecules", *Int. J. Biol. Biomed. Eng.* 9, 2015, pp. 65-74.
- [40] P. Heřman, D. Zapletal, "Modeling of Absorption and Steady State Fluorescence Spectra of Full LH2 Complex (B850 - B800 Ring)", *Int. J. Math. Mod. Meth. Appl. Sci.* 9, 2015, pp. 614-623.
- [41] W. M. Zhang, T. Meier, V. Chernyak, S. Mukamel, "Exciton-migration and three-pulse femtosecond optical spectroscopies of photosynthetic antenna complexes", *J. Chem. Phys.* 108, 1998, pp. 7763-7774.
- [42] S. Mukamel, *Principles of nonlinear optical spectroscopy*. New York: Oxford University Press, 1995.
- [43] V. I. Novoderezhkin, D. Rutkauskas, R. van Grondelle, "Dynamics of the emission spectrum of a single LH2 complex: Interplay of slow and fast nuclear motions", *Biophys. J.* 90, 2006, pp. 2890-2902.
- [44] A. G. Redfield, "The Theory of Relaxation Processes", *Adv. Magn. Reson.* 1, 1965, pp. 1-32.
- [45] D. Rutkauskas, V. Novoderezhkin, R. J. Cogdell, R. van Grondelle, "Fluorescence spectroscopy of conformational changes of single LH2 complexes", *Biophys. J.* 88, 2005, pp. 422-435.
- [46] D. Rutkauskas, V. Novoderezhkin, R. J. Cogdell, R. van Grondelle, "Fluorescence spectral fluctuations of single LH2 complexes from *Rhodospseudomonas acidophila* strain 10050", *Biochemistry* 43, 2004, pp. 4431-4438.
- [47] V. May, O. Kühn, *Charge and Energy Transfer in Molecular Systems*. Berlin: Wiley-WCH, 2000.
- [48] O. Zerlauskienė, G. Trinkunas, A. Gall, B. Robert, V. Urboniene, "Static and Dynamic Protein Impact on Electronic Properties of Light-Harvesting Complex LH2", *J. Phys. Chem. B* 112, 2008, pp. 15883-15892.
- [49] P. Heřman, I. Barvák, D. Zapletal, "Energetic disorder and exciton states of individual molecular rings", *J. Lumin.* 119-120, 2006, pp. 496-503.
- [50] P. Heřman, D. Zapletal, I. Barvák, "Lost of coherence due to disorder in molecular rings", *Phys. Stat. Sol. C* 6, 2009, 89-92.